Electrochemical and Solid-State Letters, **4** (6) A78-A81 (2001)
1099-0062/2001/4(6)/A78/4/$7.00 © The Electrochemical Society, Inc.

Layered-to-Spinel Phase Transition in Li_xMnO_2

J. Reed, G. Ceder,*,z and A. Van Der Ven

Department of Materials Science and Engineering and Center for Materials Science and Engineering, Massachusetts Institute of Technology, Cambridge, Massachusetts 02139, USA

Ab initio calculations suggest that partially lithiated layered Li_xMnO_2 transforms to spinel in a two-stage process. In the first stage, a significant fraction of the Mn and Li ions rapidly occupy tetrahedral sites, forming a metastable intermediate. The second stage involves a more difficult coordinated rearrangement of Mn and Li ions to form spinel. This behavior is contrasted to Li_xCoO_2. The susceptibility of Mn for migration into the Li layer is found to be controlled by oxidation state, which suggests various means of inhibiting the transformation. These strategies could prove useful in the creation of superior Mn-based cathode materials.
 [DOI: 10.1149/1.1368896]

Manuscript received January 8, 2001. Available electronically April 12, 2001.

Lithium manganese oxide in the α-$NaFeO_2$ layered structure is promising as an inexpensive and nontoxic positive electrode material for use in rechargeable lithium batteries.[1,2] Layered $LiMnO_2$ exhibits a smoother voltage profile and has a higher lithium content than other lithium manganese oxide structures such as spinel. Unfortunately, all pure or lightly doped layered forms of $LiMnO_2$ have been found to transform to a defective spinel-like form upon cycling in a battery with significant change in voltage profile.[3-6] In contrast, the similar $LiCoO_2$ [7,8] compound does not readily transform from layered to spinel[7] even though such a transformation is thermodynamically favored in both Li_xMnO_2 and Li_xCoO_2.[9,10] This suggests these two materials differ in performance due to kinetic rather than thermodynamic factors.

Both the layered and spinel crystal structures are characterized by the same ABC close-packed oxygen stacking sequence[1] so that a transformation between them can leave the oxygen framework unchanged. In the layered $R\bar{3}m$ α-$NaFeO_2$ crystal structure, the interstitial sites of the oxygen sublattice are occupied by Li and M atoms in alternating (111) planes. The symmetry is reduced to monoclinic $C2/m$ in $LiMnO_2$ due to a collective Jahn-Teller distortion. In going from layered $Li_{1/2}MnO_2$ to spinel, one-fourth of all Mn ions migrate into the lithium layer to what become 16d positions of spinel, while the lithium ions move to tetrahedral sites that become 8a positions of spinel.

In this paper we argue, based on the results of first principles calculations, that the transformation from layered Li_xMnO_2 to spinel-like material proceeds in two stages. In the first stage, which occurs when the material is partially delithiated, a fraction of the Mn ions in layered Li_xMnO_2 rapidly migrate to adjacent tetrahedral sites in the lithium planes. This is accompanied by roughly an equal amount of lithium ions entering tetrahedral sites on the opposite side of the octahedral vacancies left behind by the migrating Mn. We refer to tetrahedrally coordinated Li and Mn facing each other across an octahedral vacancy in the Mn plane as a ''Li-Mn dumbbell'' (Fig. 1a). The activation barrier for Mn moving tetrahedral (provided a Li trivacancy surrounds the tetrahedral site) is calculated to be quite low (0.2 eV), and is assisted by a charge-disproportionation reaction to which Mn^{+3} is prone[11]

$$2M^{+3}_{\text{oct}} \rightarrow M^{+2}_{\text{tet}} + M^{+4}_{\text{oct}} \qquad [1]$$

In the second stage of the layered to spinel transformation, the tetrahedral Mn ions and the remaining octahedral Li ions perform a coordinated rearrangement to form the final spinel phase. Stage 2 is predicted to be slower than stage 1 due to its complexity and higher activation barriers.

The above picture for the layered-to-spinel transformation is drawn from density functional theory calculations within the generalized gradient approximation using ultrasoft pseudopotentials as implemented in VASP[12] which has been shown to give good results in these systems.[13] Transition states for ion migration were calculated in periodic supercells with either 12 or 32 primitive Li_xMO_2 ($0 \leqslant x \leqslant 1$) unit cells. A $2 \times 2 \times 2$ or $1 \times 1 \times 1$ k-point mesh was used for calculations in the large supercells and a $4 \times 4 \times 4$ k-point mesh was used for calculations in cells with a $Li_xM_4O_8$ ($0 \leqslant x \leqslant 4$) formula unit.

We calculated the energies along several plausible Mn diffusion paths leading from a layered configuration to a spinel-type configu-

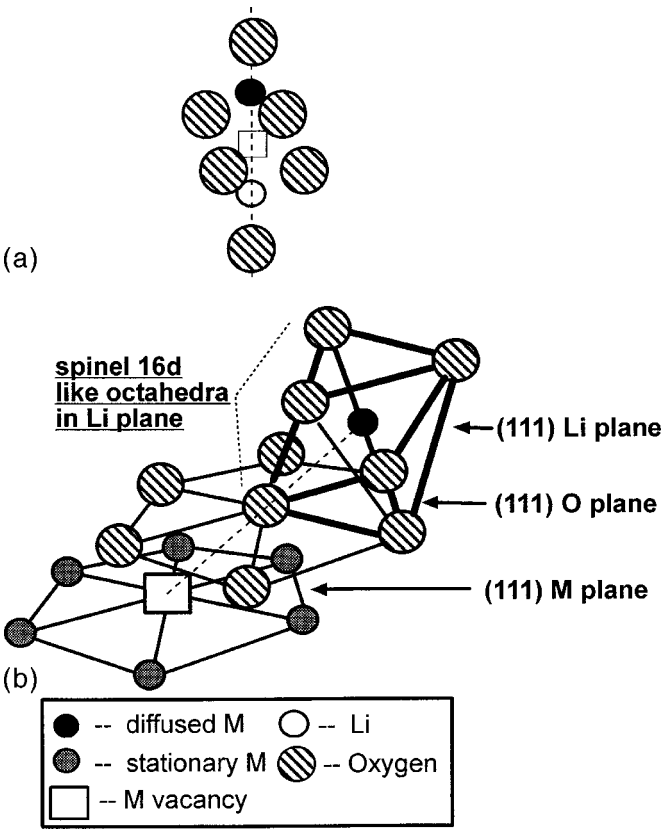

Figure 1. (a) Tetrahedral Li and M in the Li layer on each side of a M layer vacancy. (b) Pictured is a ''spinel nucleus'' with Li not shown. Li occupy tetrahedra in the Li layer on each side of the transition metal plane vacancy, *i.e.*, a ''Li-Li dumbbell''. The transformation diffusion path leads from an M layer octahedron to a Li layer octahedron 180° opposite the starting M layer position relative to one of the octahedral coordinating oxygens.

* Electrochemical Society Active Member.
z E-mail: gceder@mit.edu

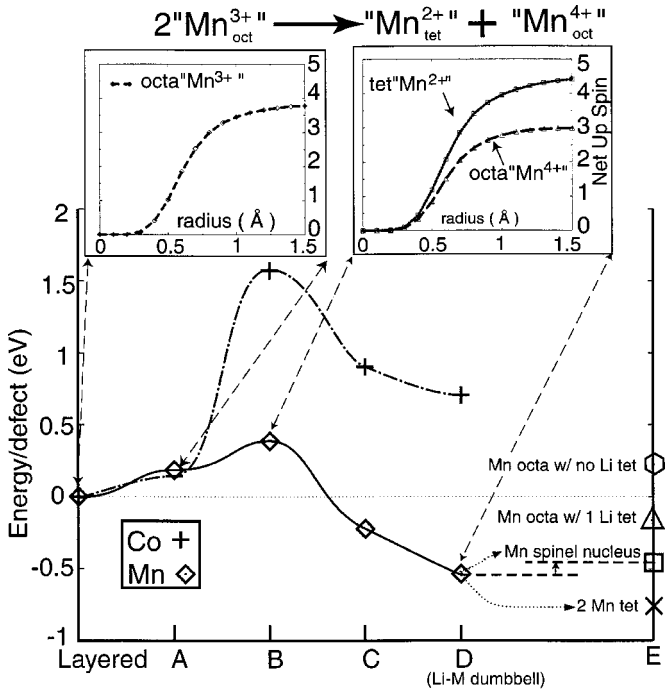

Figure 2. (A) Layered-Undefected layered structure. (B) Li rearrangement to open space for M_{tet}. (C) M defect in shared face between M layer octahedron and Li layer tetrahedron (transition state). (D) M defect in Li layer tetrahedron. Li-M dumbbell - see Fig. 1a. (E) Lowest energy is two tetrahedral Mn defects. Next lowest energy is a spinel nucleus. (Mn octahedral, 2 Li tetrahedral). Also included are energies for Mn in Li layer octahedron with 1 Li and 0 Li tetrahedral. The trend early in the transformation is for further evolution of tetrahedral Mn defects. (Insets) Integrated net spin for various types of Mn cations. (Left) 1/2 of the Mn in layered and structure ''A'' are Jahn-Teller ions with valence near +3 as shown. 1/2 are Mn^{4+} not shown. No Mn^{2+} are present in Layered or ''A''. (Right) The Mn defect (triangular coordination in ''B'', tetrahedral in ''C'' and ''D'') has a valence between +2 and +3. Such a defect gives rise to an additional Mn^{4+}_{oct} in the Mn layer.

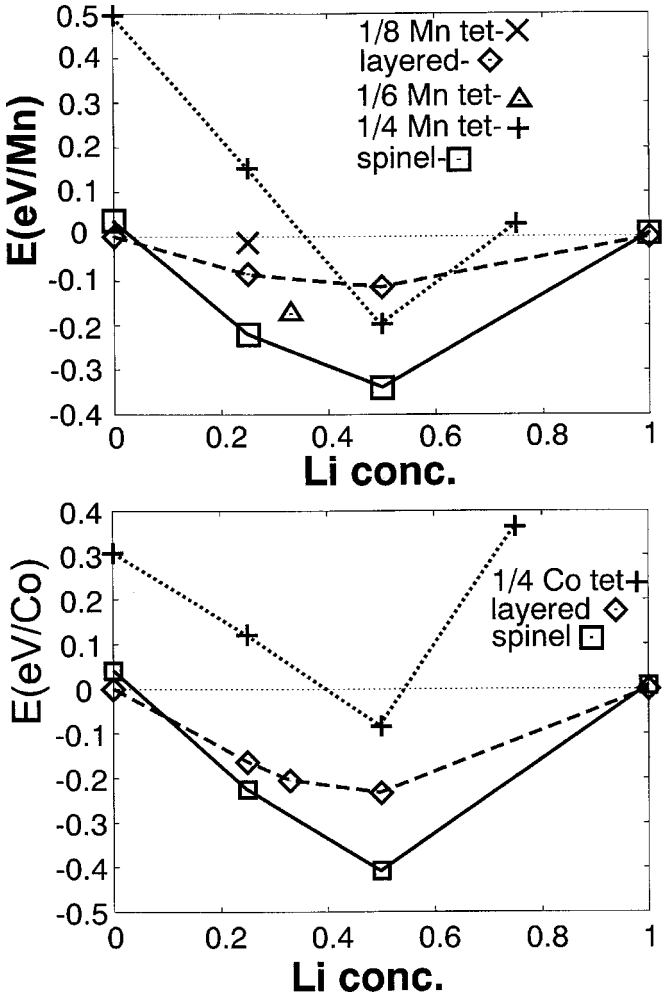

Figure 3. Energy *vs.* Li concentration for three structures of Co oxide and Mn oxide: spinel, layered, and a partially inverse spinel structure with one-quarter M tetrahedral. Note that the one-quarter Mn_{tet} structure is higher *E* than one-quarter Co_{tet} when totally dilithiated (all M^{4+}). However with addition of Li the one-quarter Mn_{tet} structure drops much more rapidly in *E* than the Co equivalent due to the favorability of charge disproportionation. The one-quarter Mn_{tet} structure goes below the layered structure energy in the vicinity of Li = 0.5 where the Mn^{2+}_{tet} state can be completely adopted, while the one-quarter Co_{tet} structure is never lower in energy then layered. Above Li = 0.5 both M_{tet} structures rises rapidly in energy due to cation repulsion. At Li = 1 tetrahedral *M* is unstable, being forced back into *M* layered.

ration or ''spinel nucleus'' illustrated in Fig. 1b. These included direct octahedral-octahedral hops, as well as hops through intermediate tetrahedral sites. The lowest energy path calculated for both Mn and Co starts with a hop from a transition metal-layer octahedron to an adjacent lithium-plane tetrahedron through the triangular face shared by the two sites. Figure 2 illustrates the energy for this hop at $x_{Li} = 0.5$ (the Li concentration at which the spinel is most thermodynamically favored over layered in both Li_xMnO_2 and Li_xCoO_2).[9,10]

If a Li layer tetrahedron is surrounded by Li vacancies, the activation barrier for a neighboring octahedral Mn to move into that tetrahedron, through the intervening triangular oxygen face, is 0.2 eV; lower than typical activation barriers for lithium diffusion in these layered materials[14] (the energetic cost of forming a Li trivacancy at $x_{Li} = 1/2$ is also about 0.2 eV). Figure 2 shows that the tetrahedral Mn defect (state C) is energetically favored over the undefected layered structure at this Li concentration. Associated with Mn passage through triangular and tetrahedral coordination is the charge-disproportionation reaction Eq. 1 as illustrated by the insets in Fig. 2. These show the integrated electron spin around a Mn nucleus as a function of the integration radius. For a high spin ion, such as Mn, total electron spin is one of the best measures of valence shifts in an *ab initio* calculation. The layered structure at $x_{Li} = 1/2$, is half Mn^{3+} and half Mn^{4+}, but only Mn^{3+} is shown in the left inset because Mn^{4+} does not contribute electrons in the formation of divalent tetrahedral Mn. The right inset shows the spin density result when one Mn has reached the activated state where it is triangularly coordinated with oxygen. This ion gains spin, becoming more like Mn^{2+} while another octahedral Mn^{3+} becomes Mn^{4+}_{oct}. We find the divalent state is retained as the Mn ion continues into the tetrahedral site, in agreement with the mechanism proposed in Eq. 1. The energy decreases further when a Li moves tetrahedral (state D) thereby forming a Li-Mn ''dumbbell''. We calculate there is no energy barrier to this Li migration, indicating that tetrahedral Mn will almost always be accompanied by a tetrahedral Li. The energy of a ''spinel nucleus'' (Fig. 1b) formed with a single Mn and two tetrahedral Li in a layered matrix (see E in Fig. 2) is higher than the Li-Mn dumbbell state by about 0.1 eV. Hence, early in the transformation (low concentrations of tetrahedral Mn defects) there is no driving force for the Mn to proceed to a spinel-like configuration. We show later that with higher concentrations of tetrahedral Mn defects a driving force for spinel nucleation does emerge.

In contrast to $Li_{1/2}MnO_2$, the situation is qualitatively different in $Li_{1/2}CoO_2$. We find a tetrahedral Co defect in the lithium plane is

associated with the same charge disproportionation reaction as tetrahedral Mn Eq. 1, however it has a very high activation energy (1.5 eV) and it is energetically unstable (Fig. 2). This difference between $Li_{1/2}MnO_2$ and $Li_{1/2}CoO_2$ runs contrary to expectations based on ion size because the ionic radius of Co (low spin in octahedral coordination) is less than or equal to that of Mn (high spin octahedral and tetrahedral) at all relevant valence states (+2, +3, +4) and coordinations (tetrahedral and octahedral).[15] Apparently, size considerations are outweighed by other factors.

The divalent Mn ion has an electronically favored half-full, spherically symmetric d-shell ($t_{2g}^3e_g^2$),[16] which allows the formation of strong sp^2 and sp^3 bonds stabilizing the passage through the triangular tetrahedral face (activated state), and the occupation of the tetrahedral position.[17] On the other hand, tetrahedrally coordinated divalent Co does not possess an energetically favored d-shell filling ($t_{2g}^3e_g^4$), and it is not conductive to covalent bonding in triangular and tetrahedral coordination.[17] Furthermore the change in ligand field stabilization energy is far more unfavorable with the advent of tetrahedral Co^{2+} than it is with tetrahedral Mn^{2+}.

We now speculate on the details of the layered-to-spinel phase transformation in Li_xMnO_2. The concentration of tetrahedral Mn arising in the first stage is regulated by both the Mn valence and the amount of Li vacancies. Mn valence is important because we found that energetically favored insertion of Mn into tetrahedral coordination is linked to the charge-disproportionation reaction Eq. 1 which requires the presence of Mn^{3+}. Li vacancies are needed to reduce cation repulsion between Li and the tetrahedral Mn. Because an increase in Li vacancies decreases the concentration of Mn^{3+} and visa versa, the optimal composition for tetrahedral Mn production is expected to be at partial delithiation. To illustrate the competing effects of Li vacancy concentration and Mn valence on the energetics of tetrahedral Mn, the energy of a structure with one-quarter Mn tetrahedral was compared with layered and spinel over various Li contents (Fig. 3). It should be noted that different fractions of tetrahedral Mn are favored at different Li concentrations. Therefore, the fraction of tetrahedral Mn in the first stage of the transformation should not be construed as fixed, at, for example, one-quarter, but rather as a quantity that depends on lithium content and Mn residence time in the intermediate state.

The further transformation of a state with Li-Mn dumbbells to spinel is not obvious. As Fig. 2 shows, it is not energetically favorable for an isolated tetrahedral Mn to migrate to a Li layer octahedron. However, we found that as more tetrahedral Mn arises, the Li layer octahedra become more receptive to Mn, and spinel nuclei become favorable. At $x_{Li} = 0.5$, the energy change for forming a spinel nuclei when one-quarter of the Mn are tetrahedral is about −0.9 eV. Therefore, at some concentration of tetrahedral Mn between 0 and one-quarter, the single Mn spinel nucleus (Fig. 1) at this Li composition becomes strongly thermodynamically favored over a dumbbell state. One possible explanation for this change is that the emergence of Li-Mn dumbbells causes the Li layer to compress to dimensions more favorable for octahedral coordination of Mn. The calculated interslab distance across the Li layer (oxygen plane to oxygen plane) decreases from 2.89 Å in the $Li_{1/2}MnO_2$ layered structure to 2.74 Å in a $Li_{1/2}MnO_2$ structure with one-quarter Mn_{tet}. Associated with this compression is a change in average bond lengths. An octahedrally coordinated Mn defect in the Li layer of the layered structure has a calculated average Mn-O bond length of 2.14 Å, while an equivalent defect in a one-quarter Mn_{tet} structure has an average Mn-O bond length of 1.94 Å which is close to the Mn-O bond length calculated for spinel of 1.95 Å. If this one-quarter Mn_{tet} structure is a good indication of the actual intermediate Li-Mn dumbbell state, it shows that the intermediate structure serves not only as an energetically favorable pathway between layered and spinel cation configurations, but also as a bridge between layered and spinel structural dimensions.

While the spinel nuclei become energetically more favorable with increasing Li-Mn dumbbell concentration, paradoxically, the activation barriers to cation rearrangement into a spinel become more formidable. The accommodation of increasing concentrations of tetrahedral Li and Mn in the Li plane reduces the availability of diffusion paths free of major cationic repulsion. We illustrate this using a representative structure, with a high concentration of ordered Li-Mn dumbbells, derived from layered $Li_{0.5}MnO_2$ by moving one-quarter of the Mn ions and half of the Li ions into Li layer tetrahedra. This structure has $R3m$ symmetry and can also be thought of as a partially inverse spinel. Three possible paths generating a spinel nucleus in this structure are shown in Fig. 4a, all of which pass through sites with large cationic repulsion. This ordered structure with high Li-Mn dumbbell concentrations represents one extreme. At the other extreme is a structure with fewer Li and the presence of tetrahedral Mn uncoupled with tetrahedral Li. An example of a low energy path through such a structure is illustrated in Fig. 4b.

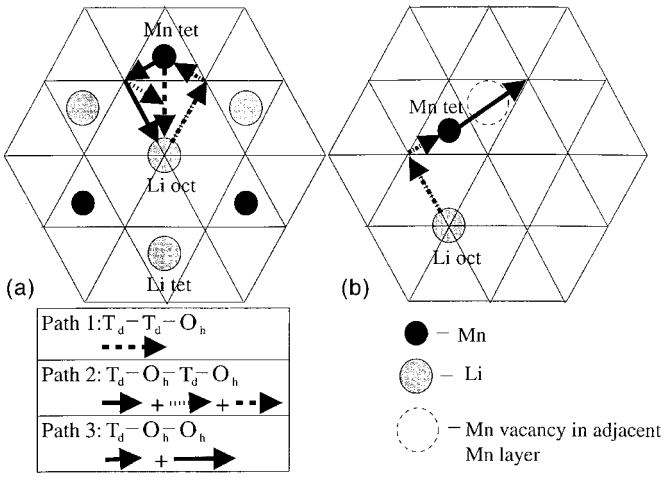

Figure 4. Looking down on a (111) Li layer. (a) Paths leading to spinel nucleus in a partially inverted (one-quarter Mn_{tet}) spinel: 1 and 2 traveling through the intervening tetrahedra suffer from polyhedra face sharing with a Mn in the Mn layer (creating a 3 eV diffusion barrier). 2 and 3 travel through an octahedra sharing a face with a Li resulting in an energy barrier of 1.5 eV. The Li residing in the 16d like octahedra must travel a path similar to 1, 2, or 3 simultaneously. (b) Low energy path to spinel nuclei in a layered structure with tetrahedral Mn defects. The face sharing Mn of the intervening tetrahedra is vacated into another Li layer tetrahedra leaving only an octahedral edge and a tetrahedral face as major diffusion barriers along this path, calculated at 0.5 and 0.3 eV. A Li must simultaneously enter the tetrahedra left by the diffusing Mn or else the energy increases 0.4 eV.

These two extreme cases suggest that a relatively gradual emergence of Li-Mn dumbbells with little ordering, would favor rapid and complete spinel creation, while a rapid formation and ordering of Li-Mn dumbbells could result in a kinetically frustrated intermediate instead of spinel. Should the proposed intermediate structure with high concentrations of Mn_{tet} at partial delithiation persist over an observable time period it would likely have the following properties

1. Symmetry will be $R\bar{3}m$ or $R3m$ if it has a defective layered structure with disordered Li-Mn dumbbells or if it assumes a partially inverted spinel-like structure as described earlier.
2. The presence of both octahedral and tetrahedral Li will make the voltage profile spinel-like but with a shortened 4 V plateau due to the occupation of some tetrahedral sites by Mn. Also the movement of Mn between tetrahedral and octahedral coordination depending on valence could increase hysteresis in the voltage profile.
3. The Jahn-Teller distortion in moderately lithiated samples will be reduced or disappear due some Jahn-Teller active Mn^{3+} being disproportionated into non-Jahn-Teller active Mn^{2+} and Mn^{4+}.

4. A major loss of capacity will result from Mn occupancy of Li layer tetrahedra, followed by a recovery of capacity as the complete spinel-like structure begins to form.

These characteristics are indeed observed in many experimental charge-discharge cyclings of layered Li_xMnO_2, which supports the existence of a persistent intermediate state of the type proposed in this paper. Many investigations[1,2,18,19] have obtained spinel-like voltage profiles but with a shortened 4 V plateau, relatively large hysteresis, and a layered-type diffraction pattern. Chiang *et al.*[20] and Hunter[21] observed reduced Jahn-Teller distortion. Chiang also observed a recovery of capacity with prolonged battery cycling, as well as the presence of substantial tetrahedral Mn in XRD and TEM studies. Choy *et al.*[22] noted a loss of inversion symmetry for some Mn in their XAS analysis, which is consistent with tetrahedral Mn.

Our proposed two-stage mechanism for the layered-to-spinel transformation recommends various strategies in designing layered compounds for greater stability. The favorable insertion of Mn in the Li layer via charge disproportionation (Eq. 1) may be inhibited by increasing the Mn^{4+}/Mn^{3+} ratio through substitution with fixed low-valence cations like Al^{3+}, Mg^{2+}, and Li^{+}, or more electronegative elements such as Co^{3+}, Cr^{3+}, or Ni^{3+}. Both mechanisms effectively reduce the electron supply needed to form Mn^{2+}_{tet} from Mn^{3+}_{oct}. The second stage may be hindered by doping with ions that do not easily move between tetrahedral and octahedral coordination, such as Co^{3+} or Cr^{3+}, which hinders the collective cation rearrangements needed to form spinel. Also, pillaring the Li layer with large cations like K^{+} would prevent the reduction of the interlayer spacing that is conducive to forming spinel nuclei. Experimentally, many of these dopings have indeed been shown to improve the stability and performance of layered Li_xMnO_2 based materials.[23-26] An example of stabilization combining two of these methods can be found in the recently introduced $Li(Cr, Mn, Li)O_2$ materials.[27] Substituting relatively electronegative Cr cations and fixed valence Li^{+} for Mn increases the Mn^{4+}/Mn^{3+} ratio, hindering migration of Mn to tetrahedral sites. Furthermore, the strong affinity of Cr cations at the oxidation levels (+2, +3, +4) for octahedral over tetrahedral sites inhibits the collective rearranging needed to form spinel. The combination of these effects explains the remarkable stability of this material.

Acknowledgments

We acknowledge support through the MRSEC Program of the National Science Foundation under award no. DMR 98-08941. G.C. acknowledges a faculty development chair from Union Miniere.

The Massachusetts Institute of Technology assisted in meeting the publication costs of this article.

References

1. A. R. Armstrong and P. G. Bruce, *Nature*, **381**, 499 (1996).
2. F. Capitaine, P. Gravereau, and C. Delmas, *Solid State Ionics*, **89**, 197 (1996).
3. A. Blyr, C. Sigala, G. Amatucci, D. Guyomard, and Y. Chabre, *J. Electrochem. Soc.*, **145**, 194 (1998).
4. Y. M. Chiang, D. R. Sadoway, Y. I. Jang, B. Huang, and H. Wang, *Electrochem. Solid-State Lett.*, **2**, 107 (1999).
5. Y. Shao-Horn, S. A. Hackney, A. R. Armstrong, P. G. Bruce, Gitzendanner, C. S. Johnson, and M. M. Thackeray, *J. Electrochem. Soc.*, **146**, 2404 (1999).
6. G. Vitins and K. West, *J. Electrochem. Soc.*, **144**, 2587 (1997).
7. K. Mizushima, P. C. Jones, P. J. Wiseman, and J. B. Goodenough, *Mater. Res. Bull.*, **15**, 783 (1980).
8. H. J. Orman and P. J. Wiseman, *Acta Crystallogr., Sect. C: Cryst. Struct. Commun.*, **139**, 12 (1984).
9. G. Ceder and A. Van der Ven, *Electrochim. Acta*, **45**, 131 (1999).
10. C. Wolverton and A. Zunger, *J. Electrochem. Soc.*, **145**, 2424 (1998).
11. R. G. Burns, *Mineralogical Applications of Crystal Field Theory*, p. 18, Cambridge University Press, Cambridge (1970).
12. G. Kresse and J. Furthmuller, *Phys. Rev. B*, **54**, 11 (1996).
13. S. K. Mishra and G. Ceder, *Phys. Rev. B*, **59**, 6120 (1999).
14. A. Van der Ven and G. Ceder, *Electrochem. Solid-State Lett.*, **3**, 301 (2000).
15. R. G. Burns, *Mineralogical Applications of Crystal Field Theory*, p. 464, Cambridge University Press, Cambridge (1970).
16. H. Bethe and R. Jackiw, *Intermediate Quantum Mechanics*, p. 80, Addison Wesley Longman, Inc., Reading, MA (1986).
17. J. B. Goodenough and A. L. Loeb, *Phys. Rev.*, **98**, 391 (1955).
18. P. Bruce, A. Armstrong, and R. Gitzendanner, *J. Mater. Chem.* (1998).
19. B. Ammundsen, J. Desilvestro, T. Groutso, D. Hassell, J. B. Metson, E. Regan, R. Steiner, and P. J. Pickering, *J. Electrochem. Soc.*, **147**, 4078 (2000).
20. H. Wang, Y. Jang, and Y.-M. Chiang, *Electrochem. Solid-State Lett.*, **2**, 10 (1999).
21. J. C. Hunter, *J. Solid State Chem.*, **39**, 142 (1981).
22. S. J. Hwang, H. S. Park, and J. H. Choy, *Chem. Mater.*, **12**, 1818 (2000).
23. Y. I. Jang, B. Y. Huang, Y. M. Chiang, and D. R. Sadoway, *Electrochem. Solid-State Lett.*, **1**, 13 (1998).
24. A. R. Armstrong, A. D. Robertson, and P. E. Bruce, *Electrochim. Acta*, **45**, 285 (1999).
25. I. J. Davidson, R. S. McMillan, J. Slegr, B. Luan, I. Kargina, J. J. Murray, and I. P. Swainson, *J. Power Sources*, **81-82**, 406 (1999).
26. M. S. Whittingham and P. Y. Zavalij, *Solid State Ionics*, **131**, 109 (2000).
27. B. Ammundsen, J. Desilvestro, R. Steiner, and P. Pickering, Abstract 17, The 10th International Meeting on Lithium Batteries, Como, Italy, May 28-June 2, 2000.